CHEMISTRY OF MATERIALS

ARTICLE

pubs.acs.org/cm

Synthetic Mechanism of Perovskite-Type $KNbO_3$ by Modified Solid-State Reaction Process

Seiji Yamazoe,*[,†] Takuya Kawawaki,[†] Kengo Shibata,[†] Kazuo Kato,[‡] and Takahiro Wada[†]

[†]Department of Materials Chemistry, Ryukoku University, Seta, Otsu 520-2194, Japan

[‡]Japan Synchrotron Radiation Research Institute, 1-1 Kouto, Sayo-cyo, Sayo-gun, Hyogo 679-5198, Japan

ABSTRACT: Perovskite-type $KNbO_3$ could be synthesized at low temperature (<600 °C) via a modified solid-state reaction method in which urea played an important role. The synthetic mechanism of $KNbO_3$ via the modified solid-state reaction process has been studied by high-temperature X-ray diffraction (HT-XRD), thermogravimetry/differential thermal analysis/mass spectrometry (TG/DTA/MS), and time-resolved energy-dispersive X-ray absorption fine structure (DXAFS) to elucidate the role of the urea. The HT-XRD showed that the urea was decomposed at 100−150 °C and $KNbO_3$ was formed at 500−550 °C via a metastable *$KNbO_3$ phase as an intermediate. From the DXAFS analysis, the structural change of the Nb_2O_5 started at 480 °C to form the perovskite-type $KNbO_3$. TG/DTA/EGA analysis showed that the urea decomposed at <400 °C. On the other hand, most $K_2C_2O_4$ was decomposed at 452−480 °C and K_2O would be generated. The formed K_2O reacted with Nb_2O_5 at 480−550 °C to form the perovskite-type $KNbO_3$, because the exothermic signal could be observed at ∼452 °C. From the above results, we propose a synthetic mechanism of perovskite $KNbO_3$ via the modified solid-state reaction process. In addition, we found that the urea contributes to the decomposition of $K_2C_2O_4$ at low temperatures.

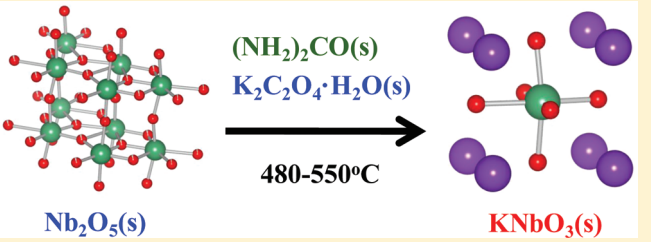

KEYWORDS: $KNbO_3$, urea, oxalate, perovskite, modified solid state reaction, XAFS, Nb K-edge

1. INTRODUCTION

$Pb(Zr,Ti)O_3$ (PZT) materials have been widely used in several applications, because of their excellent piezoelectric properties. However, PZT materials contain a large concentration of lead, which causes serious environmental problems during fabrication, use, and disposal. Therefore, it is desirable to develop lead-free piezoelectric materials with properties almost comparable to their lead-based counterparts. Among lead-free piezoelectric materials, alkali niobate families, such as $(K_{0.5}Na_{0.5})NbO_3$ (KNN) and $(Na_{0.52}K_{0.44}Li_{0.04})(Nb_{0.84}Ta_{0.10}Sb_{0.06})O_3$ (LF4), exhibit large piezoelectric constants that are comparable to that of PZT.[1−6]

Alkali niobate powders are usually synthesized via a solid-state reaction that involves heating alkaline carbonates and niobium oxide (Nb_2O_5) at high temperatures (>800 °C), because Nb_2O_5 is generally regarded as a refractory substance.[4,7−11] However, some methods enable low-temperature synthesis of the alkali niobate. The sol−gel method using niobium alkoxide and alkali alkoxide sols gave alkali niobate at 550−950 °C.[12−14] $KNbO_3$ and $NaNbO_3$ were synthesized at <200 °C via the hydrothermal synthesis method in which Nb_2O_5 reacted with alkali hydroxide aqueous solution.[15−19] Sandia octahedral molecular sieves ($Na_2Nb_{2-x}Ti_xO_{6-x}\cdot H_2O$) could be synthesized at <200 °C, using hydrothermal synthesis.[20−22] We reported that $NaNbO_3$ could be synthesized at 500−600 °C via the molten NaOH method.[23] However, these methods have some restrictions for synthesizing alkali niobate at low temperatures. In the sol−gel method, unstable alkali alkoxides and expensive niobium alkoxide must be used as starting materials. In the molten NaOH method, it is necessary to wash off excess NaOH with water. In the case of the hydrothermal synthesis, high-pressure conditions are required, although alkali niobate could be synthesized at temperatures lower than the other methods.

Recently, Xu et al. first reported the preparation of $NaTaO_3$ at low temperatures via a modified solid-state reaction method.[24] In addition, we reported that lead-free piezoelectric compounds—$KNbO_3$, $(K_{0.5}Na_{0.5})NbO_3$, and $(Na_{0.52}K_{0.44}Li_{0.04})(Nb_{0.84}Ta_{0.10}Sb_{0.06})O_3$ (LF4)—could be synthesized at 500−600 °C via the modified solid-state reaction method.[5,6,25] A similar study was reported by Chaiyo et al. in the synthesis of $(K_{0.5}Na_{0.5})NbO_3$.[26] In the modified solid-state reaction, alkali oxalate is used as a starting material and urea is used as an additive. Xu et al. reported that the added urea plays an important role.[24] Their proposed synthetic mechanism of $NaTaO_3$ via the modified solid-state reaction is described as follows:

$$Ta_2O_5 + CO(NH_2)_2 \rightarrow Ta[CO(NH)_2]_x + H_2O \quad (1)$$

$$Na_2C_2O_4 + CO(NH_2)_2 \rightarrow Na[CO(NH)_2]_x + H_2O \quad (2)$$

$$CO(NH_2)_2 + O_2 \rightarrow NH_3 + CO_2 + H_2O \quad (3)$$

$$Ta[CO(NH)_2]_x + Na[CO(NH)_2]_x + O_2 \rightarrow NaTaO_3 + NH_3 + CO_2 + H_2O \quad (4)$$

Received: June 15, 2011
Revised: August 4, 2011
Published: September 26, 2011

dx.doi.org/10.1021/cm2016966 | *Chem. Mater.* 2011, 23, 4498–4504

The urea melts at 135 °C, and the molten urea reacts with Ta_2O_5 (reaction 1) and $Na_2C_2O_4$ (reaction 2) to form Ta-complex and Na-complex, respectively. Meanwhile, the combustion of urea (reaction 3) generates much heat and results in an instantaneous high local temperature. This generated heat will be sufficient to form the $NaTaO_3$ (reaction 4). This synthesis process is simple and does not require unstable and expensive starting materials, the removal of excess alkali hydroxide after the reaction, or a high-pressure reaction chamber. However, they did not confirm the formation of the Ta-complex and Na-complex. Moreover, they did not investigate the reaction temperature at each step. The elucidation of the reaction mechanism in detail is important to understand why the modified solid-state reaction proceeds at low temperatures.

In this study, $KNbO_3$ was synthesized by the modified solid-state reaction. The synthesis process was studied by high-temperature X-ray diffraction (HT-XRD), thermogravimetry/differential thermal analysis/mass spectrometry (TG/DTA/MS), and time-resolved energy-dispersive X-ray absorption fine structure (DXAFS) to investigate the synthetic mechanism. On the basis of our results, we proposed a new synthetic mechanism of $KNbO_3$ via the modified solid-state process.

2. EXPERIMENTAL SECTION

The $KNbO_3$ (KN) was synthesized via the modified solid-state reaction method. The potassium oxalate [$K_2C_2O_4 \cdot H_2O$] (99%), Nb_2O_5 (99.9%) and urea [$CO(NH_2)_2$] (99%) were weighed at a molar ratio of [K]:[Nb]:[$CO(NH_2)_2$] = 1:1:1. These starting compounds were mixed using an agate mortar and pestle for 1.5 h. The mixture was calcined at various temperatures for 4 h in air. The obtained powder was analyzed by X-ray diffraction (XRD) (Rigaku Model RINT 2400 X-ray diffractometer, using Cu Kα radiation).

To identify the intermediate phases during the synthesis process, HT-XRD measurement was performed, using the Rigaku RINT 2400 system. The mixture of $K_2C_2O_4 \cdot H_2O$, Nb_2O_5, and urea was heated at a rate of 2 °C/min in air and XRD patterns were recorded at 25, 50, 100, 150, 200, 250, 300, 350, 400, 450, 500, 550, 600, and 650 °C. During the HT-XRD measurements, the heating was stopped and the temperatures were kept constant.

To investigate the local structural change of Nb atom during the modified solid-state reaction, the Nb K-edge DXAFS measurement was carried out. Nb K-edge DXAFS was recorded at the BL28B2 beamline in the SPring-8 facility at the Japan Synchrotron Radiation Research Institute (JASRI; 8 GeV, 100 mA). A bent Si(422) polychromator and a position-sensitive CCD detector were used to record the DXAFS spectra. The mixture of $K_2C_2O_4 \cdot H_2O$, Nb_2O_5, and urea was heated at a rate of 5 °C/min and DXAFS spectra were recorded every 2 °C. The time resolution was 0.9 s. In addition, Nb K-edge X-ray absorption fine structure (XAFS) analysis of the reference samples (Nb foil for energy calibration, Nb_2O_5, and $KNbO_3$) was also recorded at the BL01B1 beamline in the SPring-8 facility at JASRI in a transmission mode with double-crystal Si(311) monochromator and ion chambers. Data reduction was performed using the REX 2000 program Ver. 2.5.9 (Rigaku Co.).

The TG/DTA/MS analyses (Bruker, Model TG-DTA-2000SA) were carried out under the modified solid-state reaction. The mixture of $K_2C_2O_4 \cdot H_2O$, Nb_2O_5, and urea was placed in a platinum pan and heated at a rate of 2 °C/min under a 20% O_2 (diluted by N_2) atmosphere. The flow rate of the 20% O_2 gas was 50 mL/min. The α-Al_2O_3 was used as a reference sample in the TG/DTA analysis.

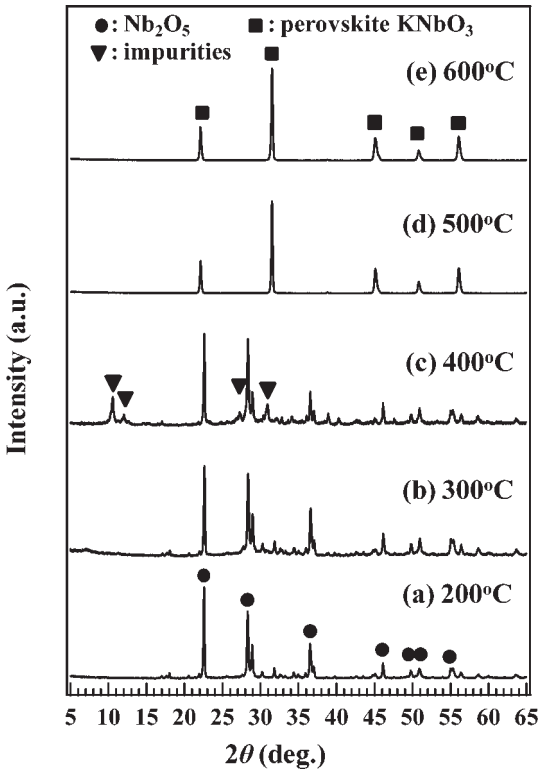

Figure 1. X-ray diffraction (XRD) patterns of the mixture of $K_2C_2O_4 \cdot H_2O$, Nb_2O_5, and urea with a molar ratio of [K]:[Nb]:[$CO(NH_2)_2$] = 1:1:1 heated for 4 h at 200 °C (pattern (a)), 300 °C (pattern (b)), 400 °C (pattern (c)), 500 °C (pattern (d)), and 600 °C (pattern (e)).

3. RESULTS AND DISCUSSION

3.1. X-ray Diffraction (XRD) Study. Figure 1 shows the XRD patterns of the heated mixture of $K_2C_2O_4 \cdot H_2O$, Nb_2O_5, and urea with a molar ratio of [K]:[Nb]:[$CO(NH_2)_2$] = 1:1:1 at 200−600 °C. The XRD patterns showed that Nb_2O_5 with T-phase[27−29] remained in the samples that were heated at 200 and 300 °C. In the sample heated at 400 °C, not only were the diffraction peaks assigned to the Nb_2O_5 observed, but unidentified diffraction peaks also were observed (at 2θ = 10.56°, 12.06°, 17.06°, and 27.24°). These diffractions would be derived from the compounds generated from the reaction between the urea and potassium oxalate, because the Nb_2O_5 did not react at 400 °C (see the DXAFS results). The $KNbO_3$ (space group *Amm*2, identified from the Inorganic Crystal Structure Database (ICSD No. 9533)) with a perovskite structure could be synthesized at a temperature above 500 °C and no impurity phases could be observed. In the case of the conventional solid-state reaction method, the perovskite-type $KNbO_3$ could be synthesized by heating above 800 °C. Therefore, the modified solid-state reaction using alkali oxalate and the urea is suitable for synthesizing the perovskite $KNbO_3$ at low temperatures.

Figure 2 shows the HT-XRD patterns of the mixture of $K_2C_2O_4 \cdot H_2O$, Nb_2O_5, and urea with a molar ratio of [K]:[Nb]:[$CO(NH_2)_2$] = 1:1:1 at 200−600 °C measured at high temperatures. Before heating, the presence of the Nb_2O_5

dx.doi.org/10.1021/cm2016966 |*Chem. Mater.* 2011, 23, 4498–4504

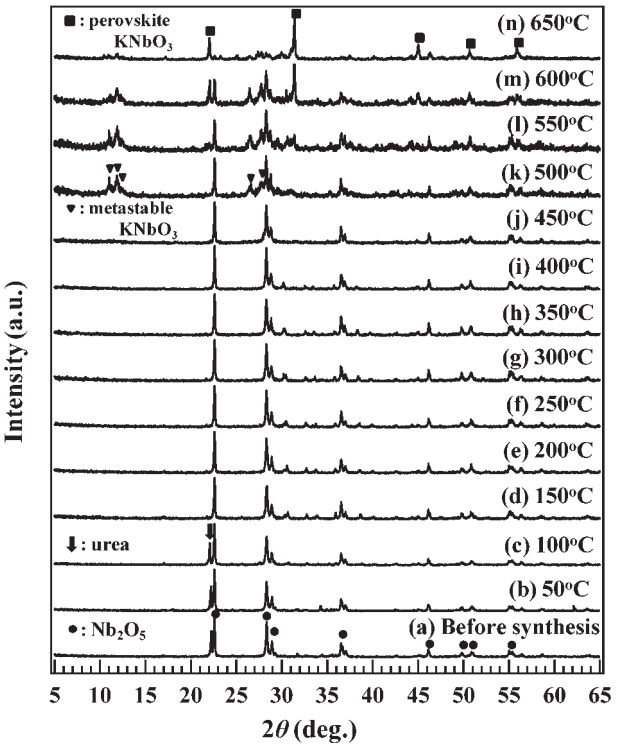

Figure 2. X-ray diffraction (XRD) patterns of the mixture of $K_2C_2O_4 \cdot H_2O$, Nb_2O_5, and urea with a molar ratio of $[K]:[Nb]:[CO(NH_2)_2]$ = 1:1:1 before heating (pattern (a)) and upon heating (measured at 50 °C (pattern (b)), 100 °C (pattern (c)), 150 °C (pattern (d)), 200 °C (pattern (e)), 250 °C (pattern (f)), 300 °C (pattern (g)), 350 °C (pattern (h)), 400 °C (pattern (i)), 450 °C (pattern (j)), 500 °C (pattern (k)), 550 °C (pattern (l)), 600 °C (pattern (m)), and 650 °C (pattern (n))).

and the urea, which are the starting materials, can be identified. Although the XRD pattern did not change below 100 °C, the diffraction peaks, assigned to the urea, disappeared at 150 °C (pattern (d) in Figure 2). This is because the urea melts at 132.5 °C. After that, the XRD patterns hardly change until 450 °C. New diffraction peaks appeared at 2θ = 11.02°, 11.90°, 12.48°, 26.62°, and 27.74° in the sample heated at 500 °C in pattern (k) in Figure 2. These diffractions are assigned to metastable $*KNbO_3$ (Powder Diffraction File Card No. 00-032-0821). The $*KNbO_3$ has a different crystal structure from that of the perovskite.[30] The diffraction peaks of the perovskite-type $KNbO_3$ are observed at 550 °C. The peak intensity of the perovskite-type $KNbO_3$ gradually increased, and the peak intensity of the $*KNbO_3$ and Nb_2O_5 decreased with heating. Almost all Nb_2O_5 reacted with $K_2C_2O_4$ at 650 °C to form the perovskite-type $KNbO_3$ in the HT-XRD condition. The generation of the $*KNbO_3$ before the formation of the perovskite-type $KNbO_3$ indicates that the perovskite-type $KNbO_3$ is synthesized from the Nb_2O_5 via metastable $*KNbO_3$. The metastable $*KNbO_3$ was reported in the solid-state reaction of K_2CO_3 and Nb_2O_5 at 380−470 °C.[31]

We also measured the HT-XRD patterns of the sample at 500 °C to identify the phases during the heating at 500 °C. Figure 3 shows HT-XRD patterns of the sample measured at 500 °C after heating for 0 min (pattern (a)), 30 min (pattern (b)), 60 min (pattern (c)), and 180 min (pattern (d)). The XRD pattern measured after reaching 500 °C (pattern (a) in Figure 3)

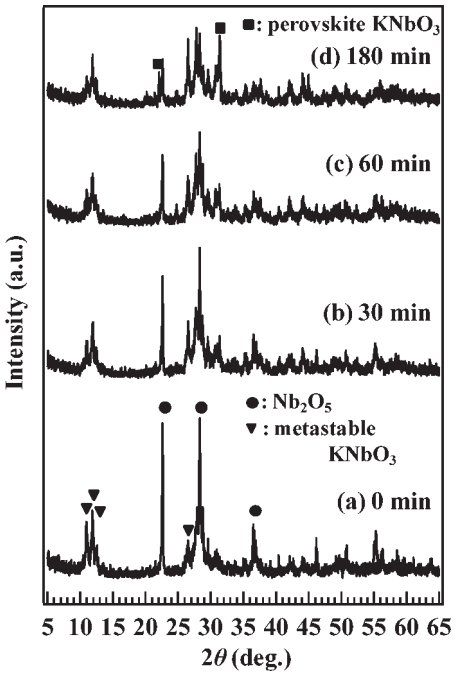

Figure 3. High-temperature X-ray diffraction (HT-XRD) patterns of the mixture of $K_2C_2O_4 \cdot H_2O$, Nb_2O_5, and urea with a molar ratio of $[K]:[Nb]:[CO(NH_2)_2]$ = 1:1:1 measured at 500 °C after 0 min (pattern (a)), 30 min (pattern (b)), 60 min (pattern (c)), and 180 min (pattern (d)).

corresponded to that in pattern (k) in Figure 2, and the metastable $*KNbO_3$ was observed. Keeping the sample at 500 °C for 30 min, the XRD pattern shown in pattern (b) in Figure 3 changed, and the formation of the perovskite-type $KNbO_3$ was confirmed. The diffraction intensity of the perovskite-type $KNbO_3$ increased with the retention time (see patterns (c) and (d) in Figure 3). Finally, the single-phase perovskite-type $KNbO_3$ could be obtained by heating at 500 °C (see Figure 1) for a prolonged time (4 h). Carriazo et al. reported that perovskite $KNbO_3$ was formed from $*KNbO_3$ at <600 °C.[32] Our results correspond to the Carriazo et al. result. Therefore, we conclude that the perovskite-type $KNbO_3$ was synthesized above 500 °C via the metastable $*KNbO_3$, using the modified solid-state reaction process.

3.2. DXAFS Study. A study using DXAFS analysis was performed on the mixture of $K_2C_2O_4 \cdot H_2O$, Nb_2O_5, and urea with a molar ratio of $[K]:[Nb]:[CO(NH_2)_2]$ = 1:1:1 to investigate the structural dynamics of the Nb atom under the modified solid-state reaction process in detail. Figure 4A shows the Nb K-edge XANES spectra measured at 25−600 °C under a modified solid-state reaction process. Moreover, Figure 4B shows the superimposed XANES spectra in the range of 19 005−19 020 eV to clarify the changes of XANES spectra. The XANES spectrum measured at 25 °C corresponded to that of pure Nb_2O_5, because Nb_2O_5 was one of the starting materials. We could not observe any significant changes of the Nb K-edge XANES spectra by heating up to 480 °C, although the intensity of the post-edge peak appearing at 19 013.2 eV slightly decreased as the temperature increased (see Figure 4B). However, Figure 4B shows that the decrease in the peak intensity stopped at 480 °C, and the peak position shifted to lower energy as the post-edge peak intensity increased. In addition, the pre-edge peak intensity slightly changed under the modified solid-state reaction. Figure 4C shows the Nb

dx.doi.org/10.1021/cm2016966 |Chem. Mater. 2011, 23, 4498–4504

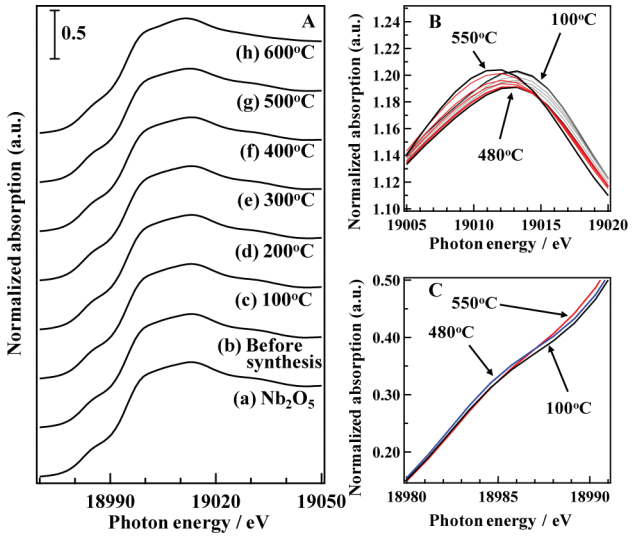

Figure 4. (A) Nb K-edge XANES spectra of Nb_2O_5 (pattern (a)), and the mixture of $K_2C_2O_4 \cdot H_2O$, Nb_2O_5, and urea with a molar ratio of $[K]:[Nb]:[CO(NH_2)_2]$ = 1:1:1 before heating (pattern (b)) and recorded after heating at 100 °C (pattern (c)), 200 °C (pattern (d)), 300 °C (pattern (e)), 400 °C (pattern (f)), 500 °C (pattern (g)), and 600 °C (pattern (h)). (B) Extended Nb K-edge XANES spectra recorded at 100−550 °C under a modified solid-state reaction. (C) Nb K-edge XANES pre-edge peaks recorded at 100, 480, and 550 °C.

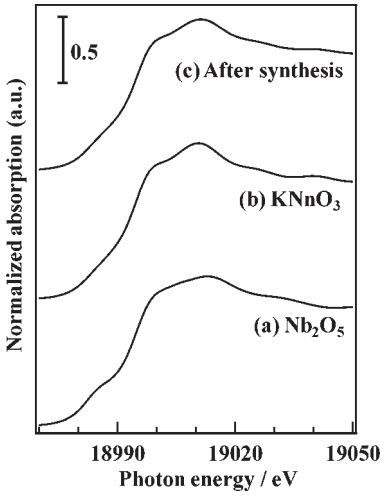

Figure 5. Nb K-edge XANES spectra of (a) Nb_2O_5, (b) $KNbO_3$, and (c) sample after modified solid-state reaction.

K-edge XANES pre-edges of the samples measured at 100, 480, and 550 °C. Increasing the temperature from 100 °C to 480 °C slightly increased the pre-edge peak intensity. However, further heating to 550 °C broadened the pre-edge peak. Shishido et al. reported that the Nb K-edge pre-edge peak intensity was dependent on the local structural symmetry of the Nb atom, because the Nb K-edge pre-edge peak is attributed to the 1s→4d electron transition.[33] If the structure of Nb is octahedral (NbO_6), the peak intensity is small. Structural distortion from an octahedron increases the pre-edge peak intensity. The T-phase Nb_2O_5 has six-coordinated NbO_6 and seven-coordinated NbO_7 species in the structure. On the other hand, $KNbO_3$ with a perovskite structure has only six-coordinated NbO_6 species (close to octahedron).

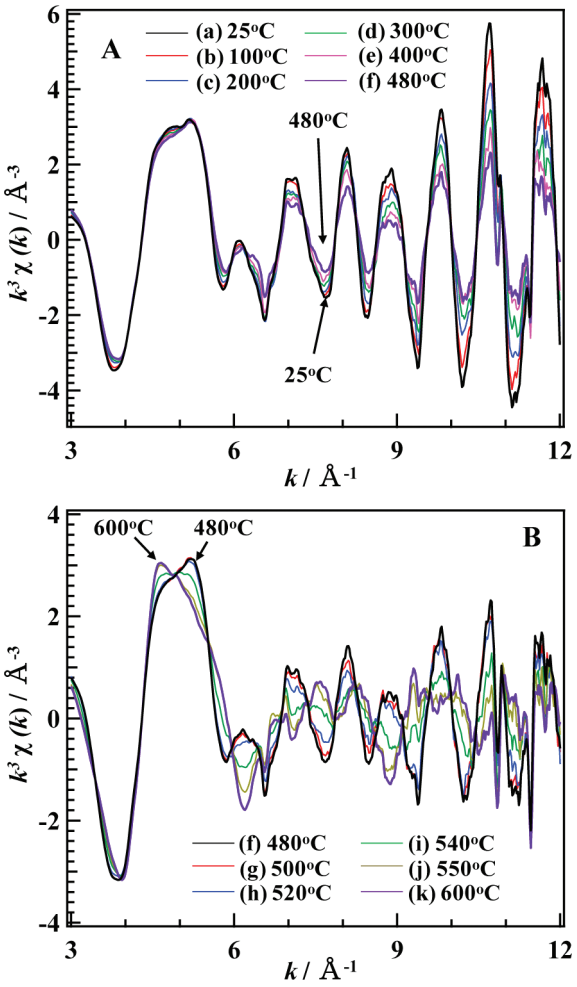

Figure 6. (A) Nb K-edge EXAFS oscillations of the sample recorded at 25 °C (trace (a)), 100 °C (trace (b)), 200 °C (trace (c)), 300 °C (trace (d)), 400 °C (trace (e)), and 480 °C (trace (f)) under modified solid-state reaction. (B) Nb K-edge EXAFS oscillations of the sample recorded at 480 °C (trace (f)), 500 °C (trace (g)), 520 °C (trace (h)), 540 °C (trace (i)), 550 °C (trace (j)), and 600 °C (trace (k)) under modified solid-state reaction.

Therefore, this broadening of the pre-edge peak is due to the structural change of the Nb atom from Nb_2O_5 to $KNbO_3$. From the results of the XANES spectra, the Nb_2O_5 begins to react at 480 °C.

After heating, the Nb K-edge XANES spectrum of the sample was recorded at room temperature. The XANES spectrum of the sample is shown in Figure 5. The XANES spectrum of the $KNbO_3$ with a perovskite structure is also shown in Figure 5. The XANES spectrum of the heated sample corresponded to that of the $KNbO_3$. Therefore, the final compound by the modified solid-state reaction is $KNbO_3$ with a perovskite-type structure.

Figure 6A shows the EXAFS oscillations measured at 25−480 °C under the modified solid-state reaction process. The EXAFS oscillation measured at 25 °C corresponded to that of Nb_2O_5 (see trace (a) in Figure 7). The oscillation pattern hardly changed up to 480 °C, although the oscillation intensity decreased in the range of 6−10 $Å^{-1}$. The decrease in the oscillation intensity is due to the increase in the Debye−Waller factor by heating. This result indicates that the structure of

dx.doi.org/10.1021/cm2016966 |Chem. Mater. 2011, 23, 4498–4504

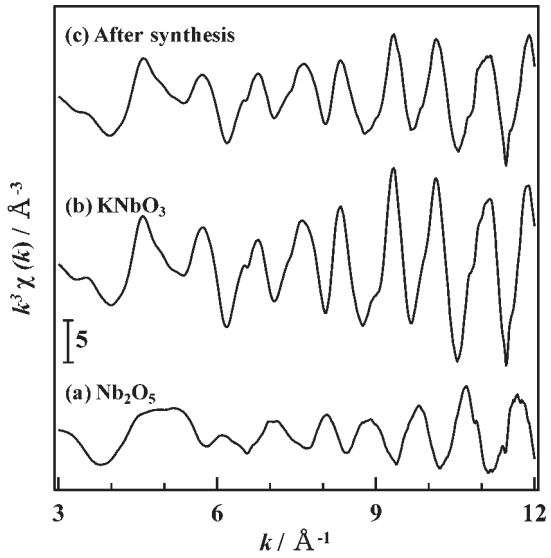

Figure 7. Nb K-edge EXAFS oscillations of Nb_2O_5 (trace (a)), $KNbO_3$ (trace (b)), and sample (trace (c)) after modified solid-state reaction.

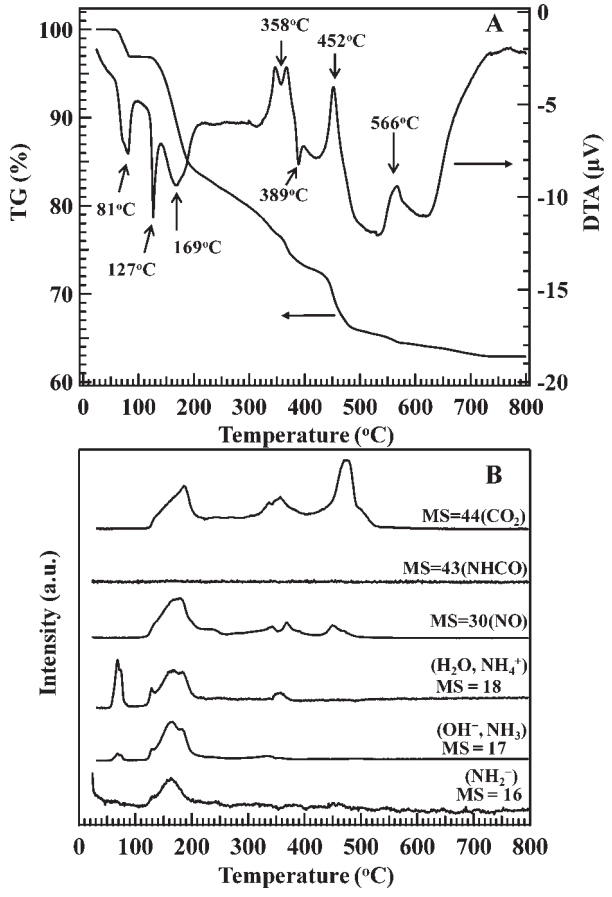

Figure 8. TG/DTA/MS data measured under 20% O_2 (N_2 balance) gas atmosphere: (A) TG/DTA data of the sample (mixture of $K_2C_2O_4 \cdot H_2O$, Nb_2O_5, and $(NH_2)_2CO$) and (B) MS data of the sample (mixture of $K_2C_2O_4 \cdot H_2O$, Nb_2O_5, and $(NH_2)_2CO$).

Nb_2O_5 does not change up to 480 °C. The result is consistent with the results obtained from the HT-XRD and the XANES studies. Figure 6B shows the EXAFS oscillations measured at 480−600 °C. The oscillation pattern began to vary at 500 °C, and a great alteration occurred in the range of 530−550 °C. This change clearly showed the local structural change of the Nb atom. After heating, we measured the Nb K-edge EXAFS oscillation of the sample at room temperature, and this spectrum is shown in Figure 7. The oscillation pattern of the heated sample corresponded to that of the perovskite-type $KNbO_3$ (trace (b) in Figure 7). This result indicates that the final compound obtained from the modified solid-state reaction is perovskite-type $KNbO_3$. The result is consistent with the result obtained from the XANES study.

3.3. TG/DTA/MS Study. TG/DTA/MS analysis was carried out on the mixture of $K_2C_2O_4 \cdot H_2O$, Nb_2O_5, and urea with a molar ratio of [K]:[Nb]:[$CO(NH_2)_2$] = 1:1:1 to investigate the mechanism of the modified solid-state reaction process in detail. Figures 8A and 8B show the TG/DTA and MS data during the modified solid-state reaction of the $KNbO_3$. The weight loss (3.1%) and endothermic peak were observed at 60−90 °C. Kamiya et al. reported that the hydration water of $K_2C_2O_4 \cdot H_2O$ is evolved at <100 °C.[34] From the MS analysis in Figure 8B, molecules with masses of 17 and 18 were detected (none with a mass of 16 was detected). This result indicates that the evolved molecule is H_2O (mass of OH^- = 17, mass of H_2O = 18). In addition, the weight loss of 3.1% corresponds to the hydration water of $K_2C_2O_4 \cdot H_2O$. Therefore, the reaction at <100 °C is the desorption of the hydration water of $K_2C_2O_4 \cdot H_2O$. The endothermic peak was observed at 127 °C. This endothermic peak is due to the melting of urea.[35]

Further heating caused a large weight loss (12.2%) with endothermic reaction at 169 °C. Chen et al. reported that the molten urea involves the following reactions in the range of 130−200 °C:[35]

$$2(NH_2)_2CO \rightarrow NH_2{-}CO{-}NH{-}CO{-}NH_2 + NH_3\uparrow \quad (5)$$

$$NH_2{-}CO{-}NH{-}CO{-}NH_2 \rightarrow \text{decomposition} \quad (6)$$

$$(NH_2)_2CO \rightarrow NHCO + NH_3\uparrow \quad (7)$$

$$3(NH_2)_2CO \rightarrow (CNOH)_3 + 3NH_3\uparrow \quad (8)$$

$$NHCO + \frac{3}{2}O_2 \rightarrow NO\uparrow + CO_2\uparrow + \frac{1}{2}H_2O\uparrow \quad (9)$$

Reaction 5 proceeds in the range of 150−170 °C with evolving NH_3. The formed $NH_2{-}CO{-}NH{-}CO{-}NH_2$ in reaction 5 decomposes at 190 °C (reaction 6). Reaction 6 occurs at 180 °C. Reaction 8 is a polymerization reaction of the urea and proceeds at >127 °C. In reaction 8, NH_3 is generated. The urea is decomposed to NHCO and NH_3 in reaction 7. From TG/DTA/MS analysis of urea (without $K_2C_2O_4 \cdot H_2O$ and Nb_2O_5), NHCO can be observed in the range of 150−200 °C. However, NHCO (mass = 43) could not be observed in the present study. Therefore, the formed NHCO is decomposed to NO, H_2O, and CO_2 (reaction 9), because a mass of 30 (NO) was detected in the temperature range of 150−200 °C. Chen et al. reported that ca. 66% weight loss of urea occurred at 150−200 °C.[35] In the present study, the weight loss is 12.2%, and this value is equal to 58% of the total weight of urea. Our result (58%)) is close to the value (66%) of Chen et al. In addition, these results were

dx.doi.org/10.1021/cm2016966 |Chem. Mater. 2011, 23, 4498–4504

supported by the MS data. Species with masses of 16, 17, 18, and 44 were detected in the range of 120−200 °C. The detected species with masses of 16, 17, and 18 correspond to NH_2^-, NH_3 and/or OH−, and NH_4^+ and/or H_2O, respectively. The species with a mass of 44 is CO_2. Therefore, evolution of NH_3 and CO_2 was confirmed. Furthermore, the shoulder peak was observed in the mass spectra of 17 and 18 at 183 °C, although this shoulder peak did not appear in the mass spectrum of 16. Therefore, this shoulder peak is H_2O. From reaction 6, the $NH_2-CO-NH-CO-NH_2$ is decomposed at 190 °C and would be formed into NH_3, CO, and so on. TG/DTA/MS analysis was carried out in the presence of O_2. Therefore, the formed CO is easily oxidized to CO_2 by O_2 in air. From the above results, approximately half of the urea is decomposed to NH_3 and CO_2 in the range of 150−200 °C.

The residual urea is polymerized above 200 °C via the following reaction:

$$6(NH_2)_2CO + \frac{3}{2}O_2 \rightarrow (CNONHCONH_2)_3 + 3NH_3\uparrow + 3H_2O\uparrow \quad (10)$$

Cheng et al. reported that the reactions 10 began to proceed at 200 °C.[35] The weight loss lasted up to 320 °C, and total weight loss of the sample in the region of 200−320 °C was 7.8%, which correspond to 37% of the weight of urea. The 37% weight loss of urea is close to the reported value. 95% of urea was decomposed up to 320 °C. Therefore, we think that the formed $(CNONHCONH_2)_3$ is decomposed to NHCO, NH_3, and CO_2 in the temperature range of 200−320 °C. The formed NHCO was decomposed by reaction 9. The residual compounds formed from urea were decomposed in the range of 320−400 °C with the endothermic reaction, according to reaction 11, as follows:

$$(CNOH)_3 \rightarrow 3HOCN \leftrightarrow 3NHCO \quad (11)$$

$(CNOH)_3$ is generated from reaction 8. HOCN and NHCO are held in equilibrium, and NHCO is decomposed by reaction 9. The weight loss in the temperature range of 100−390 °C is 22.7%, and this value is slightly larger than the weight percent of the urea (21.1%) in the sample. However, almost all urea is decomposed at <400 °C.

The endothermic peak appeared at 389 °C in Figure 8A. Kamiya et al. reported that the melting temperature of $K_2C_2O_4$ was 390 °C.[34] The peak at 389 °C is assigned to the melting point of $K_2C_2O_4$. In addition, the decomposition of $K_2C_2O_4$ occurred at 560 °C, as follows:

$$K_2C_2O_4 \rightarrow K_2CO_3 + CO\uparrow \quad (12)$$

The weight loss of $K_2C_2O_4$ is 15.2% in reaction 12. In the present study, an exothermic peak is presented at 566 °C. However, the weight loss was 1.5%, and this value corresponds to 4.6% of the weight of $K_2C_2O_4 \cdot H_2O$. The large weight loss was observed at 452 °C with an exothermic reaction. The weight loss at 452 °C was 8.5%, which is equivalent to 26.4 wt % of $K_2C_2O_4 \cdot H_2O$. Horváth and Kristóf reported that reaction 12 proceeds at 454 °C in the presence of Cr_2O_3.[36] They said this deviation can be explained by structural differences of $K_2C_2O_4$. We reported that the modified solid-state reaction does not proceed at 500 °C without urea.[25] Therefore, the urea is related to the decomposition of $K_2C_2O_4$ at 452 °C. From the TG/DTA/MS analysis, fractional compounds formed from urea remained at 389 °C, which is the melting point of $K_2C_2O_4$. Moreover, NO (mass = 30) was detected at 450−480 °C. Therefore, the residual compounds

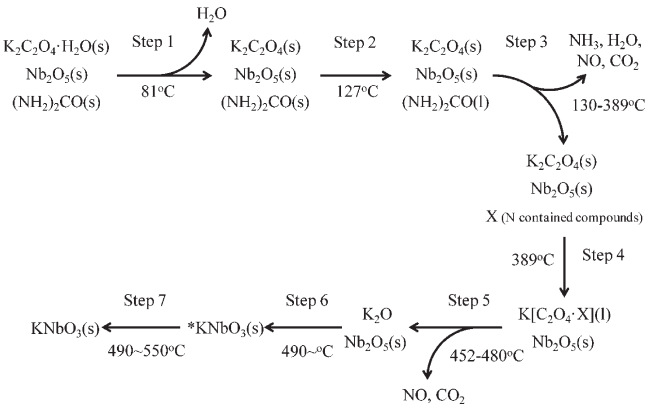

Figure 9. Synthetic mechanism of perovskite-type $KNbO_3$ via the modified solid-state reaction process.

containing N (nitrogen), such as NO_3^-, CN^- (cyanide), and so on (not NH_3, because NH_3 was not detected at 450−480 °C), affect the melted $K_2C_2O_4$ as described in the following reaction:

$$K_2C_2O_4 + X\ (\text{N-containing compounds}) \rightarrow K[C_2O_4 \cdot X] + CO_2\uparrow \quad (13)$$

In reaction 13, part of the CO_2 is desorbed from $K_2C_2O_4$, because of the coordination of X (N-containing compounds). Reaction 13 would occur at 389 K. In addition, CO_2 (mass = 44) was evolved in the range of 450−480 °C from the result of MS study (see Figure 8B). Therefore, we determined that the exothermic reaction at 430−480 °C is the decomposition of $K[C_2O_4 \cdot X]$. From the large weight loss (8.5%) in the range of 430−500 °C, the $K[C_2O_4 \cdot X]$ is decomposed to K_2O, as described by the following reaction:

$$K[C_2O_4 \cdot X] \rightarrow K_2O + NO + CO_2\uparrow \quad (14)$$

The formed K_2O reacts with Nb_2O_5 above 480 °C to form metastable *$KNbO_3$ without weight loss, as described by the following reaction:

$$K_2O + Nb_2O_5 \rightarrow 2{*}KNbO_3 \quad (15)$$

The residual $K_2C_2O_4$, which was not decomposed at 452 °C, reacted with Nb_2O_5 at 566 °C, which is the decomposition temperature of $K_2C_2O_4$, to form $KNbO_3$ as described by the following reaction:

$$K_2C_2O_4 + Nb_2O_5 + \frac{1}{2}O_2 \rightarrow 2KNbO_3 + 2CO_2\uparrow \quad (16)$$

From the weight loss (1.5%) at 566 °C, 9.7% of $K_2C_2O_4$ was not decomposed in reaction 13.

The total weight loss in the TG/DTA/MS study was 37.1%, which is reasonable, because of the theoretical value of 36.8%. Therefore, we conclude that the TG/DTA/MS data can be interpreted by a reasonable mechanism.

3.5. Synthetic Mechanism of Perovskite-Type $KNbO_3$ via Modified Solid-State Reaction. From the XRD, DXAFS, and TG-DTA/MS analyses, we proposed the synthetic mechanism of $KNbO_3$ by the modified solid-state process, as shown in Figure 9. First, hydrate water of $K_2C_2O_4 \cdot H_2O$ is desorbed at 81 °C (Step 1), demonstrated by TG-DTA analysis. The urea melts at 127 °C

dx.doi.org/10.1021/cm2016966 |Chem. Mater. 2011, 23, 4498–4504

(Step 2), observed by the results of HT-XRD and TG-DTA analysis. The polymerization (reactions 5, 8, and 10) and decomposition (reactions 6, 7, 9, and 11) of molten urea proceed in the range of 130−389 °C in Step 3. The $K_2C_2O_4$ melts at 389 °C and, at the same time, the molten $K_2C_2O_4$ reacts with the residual compounds containing nitrogen to form $K[C_2O_4 \cdot X]$ by reaction 13 (Step 4). The $K[C_2O_4 \cdot X]$ is decomposed to K_2O in the range of 452−480 °C by reaction 14 (Step 5). The formed K_2O reacts with Nb_2O_5 to form metastable $*KNbO_3$ (Step 6). The formation of $*KNbO_3$ is confirmed by HT-XRD. In addition, the structural change of Nb_2O_5 starts at 480 °C from the result of XAFS analysis. The formed metastable $*KNbO_3$ transforms to perovskite-type $KNbO_3$ in the range of 480−550 °C. Xu et al. expected that the modified solid-state reaction proceeds via reactions 1−4.[24] However, in the present study, we demonstrated that reactions 1 and 2 do not occur in the modified solid-state reaction, because almost all urea is decomposed at <400 °C without reacting with $K_2C_2O_4$ and Nb_2O_5. The role of urea in the modified solid-state reaction is the formation of N-containing compounds via the decomposition of urea in order to generate $K[C_2O_4 \cdot X]$. The decomposition of $K[C_2O_4 \cdot X]$ at 452−480 °C enables the modified solid-state reaction to proceed at low temperature of <500 °C. Therefore, we concluded that urea plays an important role for the modified solid-state reaction.

4. CONCLUSION

In this study, we elucidated the synthetic mechanism of perovskite-type $KNbO_3$ by the modified solid-state reaction process from the results of XRD, DXAFS, and TG/DTA/MS analyses. The synthetic mechanism is illustrated in Figure 9. From the TG/DTA/MS analysis, the urea is polymerized and decomposed in the temperature range of 150−400 °C. The compounds, generated from the urea, are reacted with the molten $K_2C_2O_4$ to form $K[C_2O_4 \cdot X]$. The $K[C_2O_4 \cdot X]$ is decomposed to K_2O at 452−480 °C. The formed K_2O reacts with Nb_2O_5 at 480 °C to form metastable $*KNbO_3$, which was confirmed by HT-XRD and DXAFS studies. The metastable $*KNbO_3$ transforms to perovskite-type $KNbO_3$ in the temperature range of 480−550 °C. The key reaction in the modified solid-state reaction is shown as Step 5 in Figure 9. The decomposition of $K[C_2O_4 \cdot X]$ at 452−480 °C permits low temperature (<500 °C) synthesis of perovskite-type $KNbO_3$. We demonstrated that urea plays an important role for the modified solid-state reaction at low temperatures (<500 °C).

AUTHOR INFORMATION

Corresponding Author

*Tel.: (+81) 77 543 7466. Fax: (+81) 77 543 7483. E-mail: yamazoe@rins.ryukoku.ac.jp.

ACKNOWLEDGMENT

This work was supported in part by a grant from the High-Tech Research Center Program for private universities from the Japan Ministry of Education, Culture, Sports, Science and Technology, and by Ryukoku University Joint Research Center for Science and Technology. The XAFS studies at the SPring-8 facility were carried out with the approval of the Japan Synchrotron Radiation Research Institute (JASRI) (Proposal Nos. 2008B1101, 2009A1401, 2009A1593, and 2010A1499).

REFERENCES

(1) Wada, K.; Tsuji, K.; Saito, T.; Matsuo, Y. *Jpn. J. Appl. Phys.* **2003**, *42*, 6110.
(2) Kakimoto, K.; Masuda, I.; Ohsato, H. *Jpn. J. Appl. Phys.* **2004**, *43*, 6706.
(3) Matsubara, M.; Yamaguchi, T.; Kikuta, K.; Hirano, S. *Jpn. J. Appl. Phys.* **2004**, *43*, 7159.
(4) Saito, Y.; Takao, H.; Tani, T.; Nonoyama, T.; Takatori, K.; Homma, T.; Nagaya, T.; Nakamura, M. *Nature* **2004**, *432*, 84.
(5) Fukada, M.; Saito, T.; Kume, H.; Wada, T. *IEEE Trans. Ultrason., Ferroelectr. Freq. Control* **2008**, *55*, 988.
(6) Fukada, M.; Yamazoe, S.; Wada, T. *Jpn. J. Appl. Phys.* **2009**, *48*, 091402.
(7) Domen, K.; Kudo, A.; Shibata, M.; Tanaka, A.; Maruya, K.; Onishi, T. *J. Chem. Soc., Chem. Commun.* **1986**, 1706.
(8) Qiao, H.; Xu, J.; Zhang, G.; Zhang, X.; Sun, Q.; Zhang, G. *Phys. Rev. B: Condens. Matter* **2004**, *70*, 094101.
(9) An, C.; Tang, K.; Wang, C.; Shen, G.; Qian, Y. *Mater. Res. Bull.* **2002**, *37*, 1791.
(10) Maciel, G. S.; Rakov, N.; de Araujo, C. B.; Lipovskii, A. A.; Tagantsev, D. K. *Appl. Phys. Lett.* **2001**, *79*, 584.
(11) Cho, C.-R.; Katardjiev, I.; Grishin, M.; Grishin, A. *Appl. Phys. Lett.* **2002**, *80*, 3171.
(12) Nyman, M.; Tripathi, A.; Parise, J. B.; Maxwell, R. S.; A., H. W. T.; Nenoff, T. M. *J. Am. Chem. Soc.* **2001**, *123*, 1529.
(13) Nyman, M.; Tripathi, A.; Parise, J. B.; Maxwell, R. S.; Nenoff, T. M. *J. Am. Chem. Soc.* **2002**, *124*, 1704.
(14) Camargo, E. R.; Popa, M.; Kakihana, M. *Chem. Mater.* **2002**, *14*, 2365.
(15) Zhu, H.; Zheng, Z.; Gao, X.; Huang, Y.; Yan, Z.; Zou, J.; Yin, H.; Zou, Q.; Kable, S. H.; Zhao, J.; Xi, Y.; Martens, W. N.; Frost, R. L. *J. Am. Chem. Soc.* **2006**, *128*, 2373.
(16) Goh, G. K. L.; Lange, F. F. *J. Mater. Res.* **2003**, *18*, 338.
(17) Kormarneni, S.; Roy, R.; Li, G. H. *Mater. Res. Bull.* **1992**, *27*, 13931405.
(18) Lu, C.-H.; Lo, S.-Y.; Lin, H.-C. *Mater. Lett.* **1998**, *34*, 172.
(19) Uchida, S.; Inoue, Y.; Fujishiro, Y.; Sato, T. *J. Mater. Sci.* **1998**, *33*, 5125.
(20) Pless, J. D.; Garino, T. J.; Maslar, J. E.; Nenoff, T. M. *Chem. Mater.* **2007**, *19*, 4855.
(21) Xu, H.; Navrotsky, A. *J. Mater. Res.* **2005**, *20*, 618.
(22) Nenoff, T. M.; Pless, J. D.; Michaels, E.; Phillips, M. L. F. *Chem. Mater.* **2005**, *17*, 950.
(23) Yamazoe, S.; Kawawaki, T.; Imai, T.; Wada, T. *J. Ceram. Soc. Jpn.* **2010**, *118*, 741.
(24) Xu, J.; Xue, D.; Yan, C. *Mater. Lett.* **2005**, *59*, 2920.
(25) Wada, T.; Suzuki, A.; Saito, T. *Jpn. J. Appl. Phys.* **2006**, *45*, 7431.
(26) Chaiyo, N.; Ruangphanit, A.; Muanghlua, R.; Niemcharoen, S.; Sangseub, A.; Taopen, S.; Leelapattana, S.; Vittayakorn, W. C.; Vittayakorn, N. *Ferroelectrics* **2009**, *383*, 8.
(27) Orel, B.; Maček, M.; Gradolnik, J.; Meden, A. *J. Solid State Electrochem.* **1998**, *2*, 221.
(28) Ristić, M.; Popović, S.; Musić, S. *Mater. Lett.* **2004**, *58*, 2658.
(29) Nowak, I.; Ziolek, M. *Chem. Rev.* **1999**, *99*, 3603.
(30) Nassau, K.; Wang, C. A.; Grasso, M. *J. Am. Ceram. Soc.* **1979**, *62*, 503.
(31) Flueckinger, U.; Arend, H.; Oswald, H. R. *Am. Ceram. Soc. Bull.* **1977**, *56*, 575.
(32) Carriazo, D.; Martin, C.; Rives, V. *Eur. J. Inorg. Chem.* **2006**, *2006*, 4608.
(33) Shishido, T.; Asakura, H.; Yamazoe, S.; Teramura, K.; Tanaka, T. *J. Phys.: Conf. Ser.* **2009**, *190*, 012073.
(34) Kamiya, H.; Kimura, A.; Tsukada, M.; Naito, M. *Energy Fuels* **2002**, *16*, 457.
(35) Chen, J. P.; Isa, K. *J. Mass Spectrom. Soc. Jpn.* **1998**, *46*, 299.
(36) Horváth, A.; Kristóf, J. *J. Thermal Anal.* **1990**, *36*, 1471.